

Terrestrial gamma ray flashes correlated to storm phase and tropopause height

D. M. Smith,¹ B. J. Hazelton,¹ B. W. Grefenstette,¹ J. R. Dwyer,^{2,3} R. H. Holzworth,³ and E. H. Lay⁴

Received 31 August 2009; revised 13 November 2009; accepted 4 January 2010; published 4 August 2010.

[1] We compare the seasonal and geographical occurrence of terrestrial gamma ray flashes (TGFs) with global lightning maps and find that only part of the difference can be explained by differences in tropopause altitude. The altitude hypothesis suggests either that TGFs are produced only in conjunction with the highest lightning or that only the highest events are seen from space because of the easier escape of gamma rays from the atmosphere. We find that the differences in atmospheric transmission due to seasonal and geographical differences in tropopause height play a major but not dominant role in reconciling lightning and TGF maps and that other factors are needed to explain the remaining local differences. In a second analysis, we use radio atmospherics data from the World Wide Lightning Location Network to study at what time in the evolution of a storm TGFs tend to be seen. We find that, on average, TGFs lag the peak flash rate of the associated storm by 38 min, although the range of lags is extremely wide, including some cases where the TGF leads the peak flash rate.

Citation: Smith, D. M., B. J. Hazelton, B. W. Grefenstette, J. R. Dwyer, R. H. Holzworth, and E. H. Lay (2010), Terrestrial gamma ray flashes correlated to storm phase and tropopause height, *J. Geophys. Res.*, 115, A00E49, doi:10.1029/2009JA014853.

1. Introduction

[2] While it has been known that terrestrial gamma ray flashes (TGFs) were associated with thunderstorms since their discovery [Fishman *et al.*, 1994], and, indeed, with individual lightning flashes [Inan *et al.*, 1996; Cummer *et al.*, 2005; Stanley *et al.*, 2006], little is certain beyond this general correlation. The radio atmospherics (sferics) associated with TGF lightning have been described as similar to those producing sprites (in the first case [Inan *et al.*, 1996]), as being of low charge moment (11–107 Ckm for a sample of 13 [Cummer *et al.*, 2005]), and as being, on the contrary, among the largest in peak VLF intensity in their associated thunderstorm [Inan *et al.*, 2006]. The most detailed measurements of VLF/LF waveforms, with the Los Alamos Sferic Array (LASA), show morphologies consistent with positive intracloud (+IC) flashes, including some narrow bipolar events (NBEs) [Stanley *et al.*, 2006; Shao *et al.*, 2010]. Among the open questions about TGFs are their ubiquity (whether they are associated with all lightning) and the causative relation with lightning.

[3] Relativistic runaway, first proposed by Wilson [1925], is now widely accepted to be the physical mechanism responsible for the generation of high-energy electrons and their gamma ray bremsstrahlung in thunderstorms. This process requires high electric fields, but for the TGFs these could either be quasistatic fields set up by a lightning discharge, fields due to the original separation of charge in the cloud before lightning occurs, or transient electric fields near lightning streamers and leaders [Moss *et al.*, 2006; Dwyer, 2008; Carlson *et al.*, 2009]. In the latter scenario, according to Moss *et al.* [2006], the acceleration is a two-stage process in which high fields at streamer tips accelerate a large number of seed electrons to a few keV, at which point a larger-scale but lower-strength field associated with the leader head accelerates these seeds via relativistic runaway to MeV energies. For the case of quasi-static fields (before or after lightning), the Dwyer instability, in which positron and gamma ray feedback processes cause an exponential growth of runaway avalanches, allows the relativistic process to short out the high-field region [Dwyer, 2003, 2008].

[4] High-energy radiation on a timescale of seconds to minutes, much slower than TGFs, has been observed with detectors in aircraft [Parks *et al.*, 1981; McCarthy and Parks, 1985], on balloons [Eack *et al.*, 1996a, 1996b, 2000], and on the ground [Brunetti *et al.*, 2000; Torii *et al.*, 2002; Tsuchiya *et al.*, 2007]. This is presumably due to runaway electrons generated by prelightning fields. Runaway in this process, if sufficiently amplified by feedback, could initiate lightning by creating the initial conductive channel.

¹Santa Cruz Institute for Particle Physics and Physics Department, University of California, Santa Cruz, California, USA.

²Department of Physics and Space Science, Florida Institute of Technology, Melbourne, Florida, USA.

³Department of Earth and Space Sciences, University of Washington, Seattle, Washington, USA.

⁴Los Alamos National Laboratory, Los Alamos, New Mexico, USA.

[5] The Reuven Ramaty High Energy Solar Spectroscopic Imager (RHESSI), a NASA satellite designed to study solar flares, has produced the largest available database of TGFs to date, with nearly 1000 events recorded. In the first part of this paper, we compare the RHESSI TGF database (time and location of each event) with the global record of lightning locations from the World Wide Lightning Location Network (WWLLN) [Lay et al., 2004; Rodger et al., 2006], and find that TGF production lags the peak flash rate in an average storm. In the second part, we compare the TGF occurrence maps with seasonal lightning maps from NASA's Lightning Image Sensor (LIS) and Optical Transient Detector (OTD) satellite instruments and maps of seasonal average tropopause height from the NCAR/NCEP reanalysis [Kalnay et al., 1996]. We find that only part of the difference between TGF and lightning maps can be accounted for by the effect of atmospheric absorption of gamma rays varying with storm height as approximated by average seasonal tropopause height. This idea was first suggested qualitatively by Williams et al. [2006]. We note that the same effect would appear if the TGF production mechanism required high altitudes to work, and there were no "hidden" low-altitude TGFs at all. We know of no theoretical reason to expect an altitude floor to the TGF phenomenon, however.

2. Data Sets

[6] RHESSI is in a low-Earth orbit with 38° inclination. Its germanium detectors are sensitive to atmospheric gamma rays in the range of approximately 50 keV to 20 MeV. A detailed description of RHESSI's capabilities and the TGF observations is given by Grefenstette et al. [2009]. Here we restrict our attention to the season and location of each TGF, ignoring spectral information and other characteristics. We note, however, two limitations in RHESSI's ability to recognize a TGF event. First, since the average TGF contains only about 20 individual gamma rays, we are limited in our ability to see much fainter events, since there are typically from 1 to 3 background gamma rays in any 1 ms time interval chosen at random. Second, due to dead time effects in RHESSI's electronics, TGFs on the short end of the time distribution ($\ll 200 \mu\text{s}$) might often be missed no matter how bright they are, since it is difficult for the electronics to collect 20 counts in that time. The full RHESSI database is publicly available at http://scipp.ucsc.edu/~dsmith/tgflib_public/. RHESSI has no ability to detect the direction of incoming gammas at these energies. A TGF could then have originated, in principle, anywhere within the satellite's ~ 2500 km horizon. But the few TGFs identified with specific triangulated sferics occur usually within 300 km and nearly always within 600 km of the subsatellite point. These include the events discussed by Cummer et al. [2005], Stanley et al. [2006], Hazelton et al. [2009] and Shao et al. [2010], although the distances are not always given in these papers.

[7] WWLLN [Lay et al., 2004; Rodger et al., 2006] is a lightning location network of 30+ very low frequency (VLF; 3–30 kHz) sensors operated at sites around the world. It is optimal for the identification of storms, providing continuous global coverage. Few RHESSI TGFs are directly associated with WWLLN sferics [Lay et al., 2005; Hazelton et al., 2009] probably because WWLLN is sensitive mostly

to large cloud-to-ground (CG) flashes [Rodger et al., 2008]. However, it has been shown that WWLLN is able to detect nearly all lightning-producing storms [Jacobson et al., 2006]. For information on obtaining WWLLN data, see <http://wwlln.net/>.

[8] The LIS/OTD data set provides a global view of lightning, including seasonal dependence, based on optical observations of flashes from orbit over many years. Since the satellites covered only a small portion of the Earth at any time, most individual storms were not observed, but the long-term average has been corrected for spatially and diurnally varying observing efficiencies. Maps are available on a monthly cadence, with each month averaged over many years of data. These data are available from <http://thunder.msfc.nasa.gov/data/>.

[9] Tropopause heights were estimated using the National Centers for Environmental Prediction/National Center for Atmospheric Research (NCEP/NCAR) reanalysis [Kalnay et al., 1996]. As with the LIS/OTD data, the data set we chose was that representing a multiyear average for each calendar month for each geographical position.

3. Storm-Phase Analysis

[10] We examined WWLLN lightning data in the spatial and temporal proximity of RHESSI TGFs from 2003 November (when the WWLLN attained global coverage) to 2008 July. Within this period, out of 619 TGFs, we found 51 for which there was only one well-defined WWLLN storm within 600 km of the TGF flash. For the remainder of the TGF population, there were usually several spots of activity within 600 km that might have produced the TGF. The "single-storm" criterion required at least 5 flashes within 600 km and 20 min of the TGF, and that these flashes have a root mean square (rms) spread in distance of < 100 km from their average position.

[11] To determine in what phase of the storm evolution TGFs most commonly appear, we made a histogram of flash rate as a function of time for each TGF-related storm. Figure 1 shows the sum of all 51 histograms, aligned so that each TGF occurs at $t = 0$. Within 20 min of zero (the part of the histogram marked with a bold line), all the flashes should have been related to the TGF-producing storm, based on the way our single-storm sample was constructed. There is a clear decline in flash rate during this period, suggesting that TGFs occur preferentially during the decline of flash production. Beyond ± 20 min, many of the flashes may still be from the TGF storm region but an increasing number could be from other storms within 600 km.

[12] It is difficult to evaluate the statistical significance of the result when it is presented this way, because the histogram of Figure 1 is dominated by the few most active storms. We therefore went back to the data from each storm and calculated the percent change in flash rate between the 20 min before the TGF and the 20 min after. A histogram of the percent change is shown in Figure 2; here, each count in the histogram represents a storm rather than a single flash. In 37 out of the 51 TGFs, the flash rate drops rather than increasing. Using binomial statistics, the probability of this great an imbalance occurring accidentally in either direction is only 1.8×10^{-3} . The average delay between the peak flash rate and the TGF was 38 min, but with a very large standard

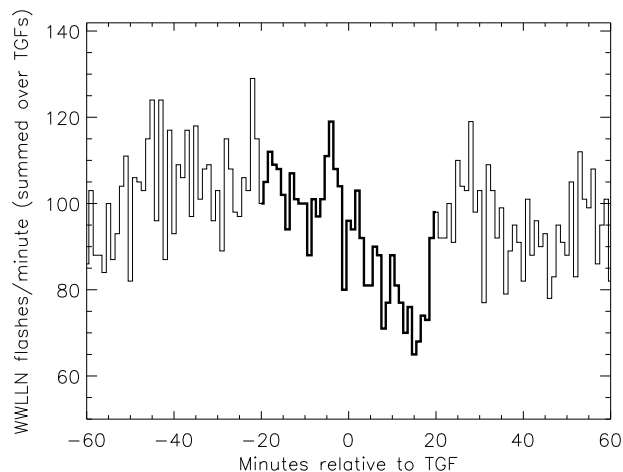


Figure 1. Summed WWLLN flash rate for all single-storm RHESSI TGFs, aligned relative to the TGF occurrence time.

deviation for the distribution of 98 min. Since these times are >20 min, this distribution is subject to contamination from unrelated storms.

3.1. Discussion

[13] The most detailed observations of lightning sferics associated with TGFs, by LASA [Stanley *et al.*, 2006; Shao *et al.*, 2010], have found only positive intracloud flashes (including some NBEs). Williams *et al.* [1989] found that the peak of IC lightning tends to lead the peak of CG lightning by 5–10 min in a typical storm. Thus it is surprising that TGFs (expected to associate with IC lightning) lag, rather than lead, the peak of WWLLN sferics (WWLLN being more sensitive to CG than IC lightning).

[14] We cannot explain this discrepancy yet, but we can outline some directions for further inquiry. First, as mentioned in the context of the mapping analysis of section 4.1, the TGFs we see from space could be only the small subset representing the highest-altitude events. If the highest-altitude subset of ICs tends to peak later than other ICs, and, indeed, later than CG lightning, our observation would be explained. We have not found any evidence of such an effect in the literature, but a natural next step would be to study infrared satellite data, and radar data when available, for the 51 isolated WWLLN storms associated with RHESSI TGFs, to see if their cloud-top height rises as they evolve.

[15] Second, it is possible that the southeastern United States plus the Caribbean is an anomalous region in terms of the type of lightning most associated with TGFs. It is from this region that come both the Duke University data showing TGFs to have associated sferics with very small charge moment change [Cummer *et al.*, 2005] and the LASA data identifying +IC flashes and NBEs with TGFs. If +CG lightning is responsible for most TGF production in other parts of the planet, we may again be able to reconcile our new result on storm phase with expectations. While this may sound unlikely, other sferic research not restricted to this local region has yielded different results: Inan *et al.* [1996], finding the first association of a sferic with a TGF, reported a large charge-moment change with a continuing current, similar to the sferics associated with sprites. Inan *et al.*

[2006], using global sferic detections from their facility at Palmer Station, Antarctica, and RHESSI TGFs, found that the sferics associated with TGFs were among the largest from the associated storm. This suggests either +CG flashes or particularly large NBEs, either of which might have a different time distribution than run-of-the-mill ICs such as those discussed by Williams *et al.* [1989].

3.2. Spatial Relation Between Storm Center and TGF

[16] In an earlier paper [Dwyer *et al.*, 2008], we showed that a small fraction of TGFs detected by satellites are actually beams of electrons launched from the top of the atmosphere at the site of the storm, following the magnetic field line to the spacecraft. This process must occur when a gamma ray flash does, since gamma rays will knock electrons off atoms in the upper layer of the atmosphere. These electron-beam detections are characterized by a long duration (several milliseconds to tens of milliseconds) caused by dispersion of electrons at different pitch angles relative to the field. Thus, most RHESSI TGFs, with durations from 200 μ s to 2 ms, are expected to be direct photon detections.

[17] We can verify this with the WWLLN and RHESSI data sets. If most TGFs were actually the detection of electrons following the magnetic field from the site of the original gamma event, then the satellite should be systematically equatorward of the parent storms. Figure 3 shows a histogram of the difference in the absolute value of magnetic latitude between the single-storm positions and the associated TGF. There is no equatorward bias, consistent with a photon nature of the TGFs, as expected.

4. Tropopause Analysis

4.1. Mapping

[18] Figure 4d shows the global distribution of RHESSI TGFs, or, rather, the distribution of the point directly below the spacecraft when the TGF occurred, since RHESSI cannot sense the direction of the incoming gamma rays. Instrumental-sensitivity effects distort this image relative to the

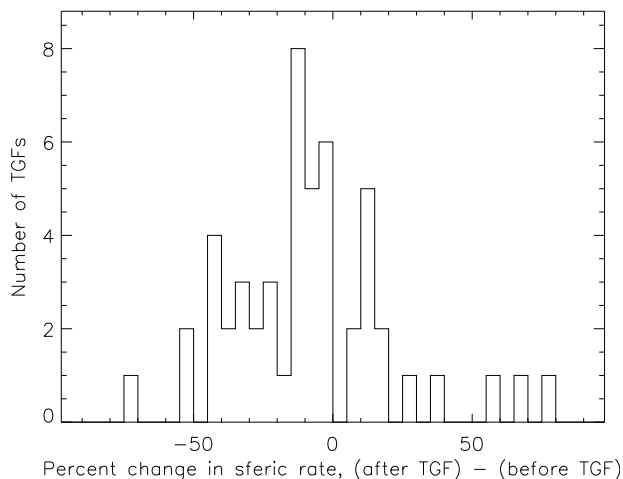


Figure 2. Histogram of the percent change in WWLLN flash rate between the 20 min before each single-storm TGF and the 20 min after.

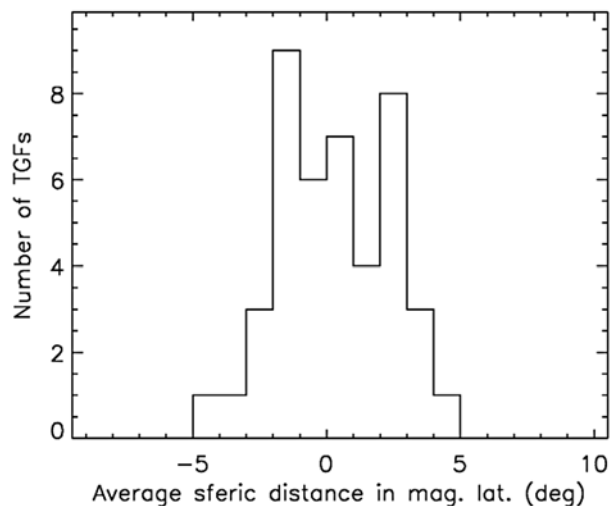


Figure 3. Distribution of the difference between the absolute values of magnetic latitude of RHESSI subsatellite positions and WWLLN-derived single-storm positions. There is no bias for the satellite to be equatorward of the storm.

true TGF map. These include the different amounts of time spent over different regions by the satellite (including a sharp cutoff at its orbital inclination of 38°), the gap over Brazil and the southern Atlantic due to the passage of the spacecraft through the South Atlantic Anomaly (SAA), the lowest part of Earth’s inner radiation belt, higher gamma ray background levels at higher magnetic latitudes, and the instrumental rejection (“decimation”) of a fixed fraction of the gamma rays in these regions of high magnetic latitude to save space on RHESSI’s onboard data recorder [Grefenstette *et al.*, 2009].

[19] We cannot invert these effects to create a true TGF map (for example, we would have no idea what to put in the regions with no exposure), but we can artificially induce these same distortions into other global distributions in order to make a direct comparison. Figure 5a is a map of the global factor (exposure \times sensitivity) by which any unbiased global map should be multiplied for comparison with the map in Figure 4d. This map was obtained by randomly adding simulated TGFs to the real RHESSI gamma ray data stream with a uniform probability in time and mapping the positions corresponding to those that were successfully detected by our TGF-detection software. There is no significant seasonal dependence to this factor.

[20] Figure 4a shows the global lightning map from LIS/OTD, and Figure 4b shows the same map after multiplication by the RHESSI exposure map in Figure 5a. All the maps in Figure 4 show the percentage of the global flash total in each pixel. While the exposure correction has certainly improved the comparison in the obvious ways (such as the lack of data in the south Atlantic), there are still large differences: for example, there is a lot of lightning in the Mediterranean and Great Plains of the United States, but almost no TGFs in these regions.

[21] Williams *et al.* [2006] suggested that, since gamma rays are absorbed by significant amounts of air, TGFs are seen primarily from the highest +IC lightning, even though they might be associated with other, lower-altitude lightning

as well. The highest storms generally occur where the tropopause is highest, which is in the tropics; thus the equatorial concentration of TGFs relative to lightning could be explained by a selection bias toward the highest-altitude TGFs.

[22] We test this hypothesis using the monthly tropopause models from the NCEP/NCAR reanalysis. Each month is generic, i.e., derived from many years of data, and not specific to the RHESSI observing years. The comparison is statistical: storms that overshoot significantly or unusual temporary deviations from typical tropopause heights cannot be modeled. The NCEP/NCAR tropopause heights are in units of mbar of pressure, but gamma ray attenuation is more directly related to the overlying mass. We use the U.S. Standard Atmosphere and the table of overlying mass versus altitude from Humphreys [1964] to derive the following approximate conversion:

$$\Sigma = 1.04173P + 5.17 \quad (1)$$

where P is pressure in mbar and Σ is overlying mass in g/cm^2 . We used GEANT3 Monte Carlo simulations to determine the effect of atmospheric absorption on a TGF. GEANT3 [GEANT Team, 1993] simulates all relevant high-energy interactions of electrons and photons with matter, including Compton scattering, photoelectric absorption, and pair production (for photons), ionization losses and bremsstrahlung (for electrons and positrons), and positron annihilation. We simulated an upward beam of electrons with an exponential energy spectrum (folding energy 7.2 MeV) to represent a typical relativistic runaway spectrum. For depths ranging from 50 to 250 g cm^{-2} of overlying air, we counted the number of photons >100 keV exiting the atmosphere. The resulting transmission factors are close to exponential with overlying mass, with a folding length of 45 g cm^{-2} .

[23] Figure 5b shows the tropopause height from the NCEP/NCAR reanalysis for the month of January, and Figure 5c shows the calculated gamma ray transmission from the tropopause to space using the exponential folding derived from GEANT. For each month, we multiplied this transmission factor by the LIS/OTD lightning map for the month. When summed over the year and corrected with the RHESSI exposure/efficiency map, this process creates a map that accounts for tropopause-height effects as well as lightning distribution. The agreement with the RHESSI TGF map is qualitatively better, with part of the TGF deficit at high latitudes reproduced.

[24] The remaining discrepancies can be seen in Figures 5d, 6 and 7. The most notable feature is a deficit of TGFs in Africa relative to the other hot spots in the Americas and the Maritime Continent (Figure 7). Other TGF deficits appear in the continental United States and a band running from northern India up through central Asia. These three areas with TGF deficits are all inland, while those with TGF excesses are rich in coastline and islands. This may suggest a climatological factor that makes nearby ocean conducive to TGF formation. See Splitt *et al.* [2010] for a discussion of specific climatological factors in the TGF context, such as liquid water content and convective available potential energy.

[25] There may also, however, be separate explanations for these different regions of TGF deficit. In the case of Africa, there may be a role for instrumental bias. RHESSI’s

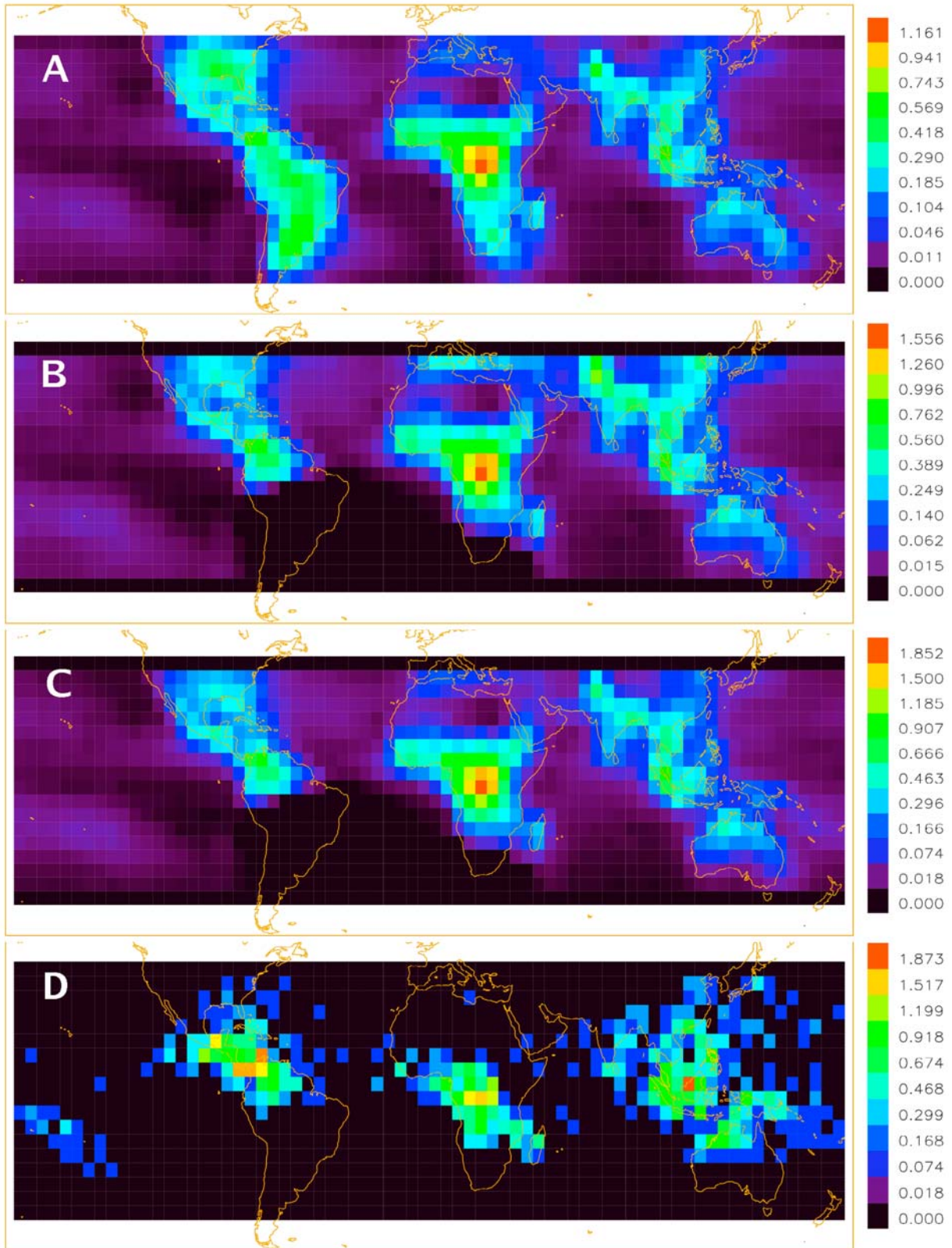


Figure 4. Lightning and TGF maps. The scale is the percentage of total flashes in each pixel. (a) NASA LIS/OTD lightning map. (b) LIS/OTD map multiplied by RHESSI exposure/efficiency map. (c) LIS/OTD monthly maps multiplied by monthly gamma ray transmission factor, summed, and, finally, multiplied by the RHESSI exposure/efficiency map. (d) RHESSI TGF detection map.

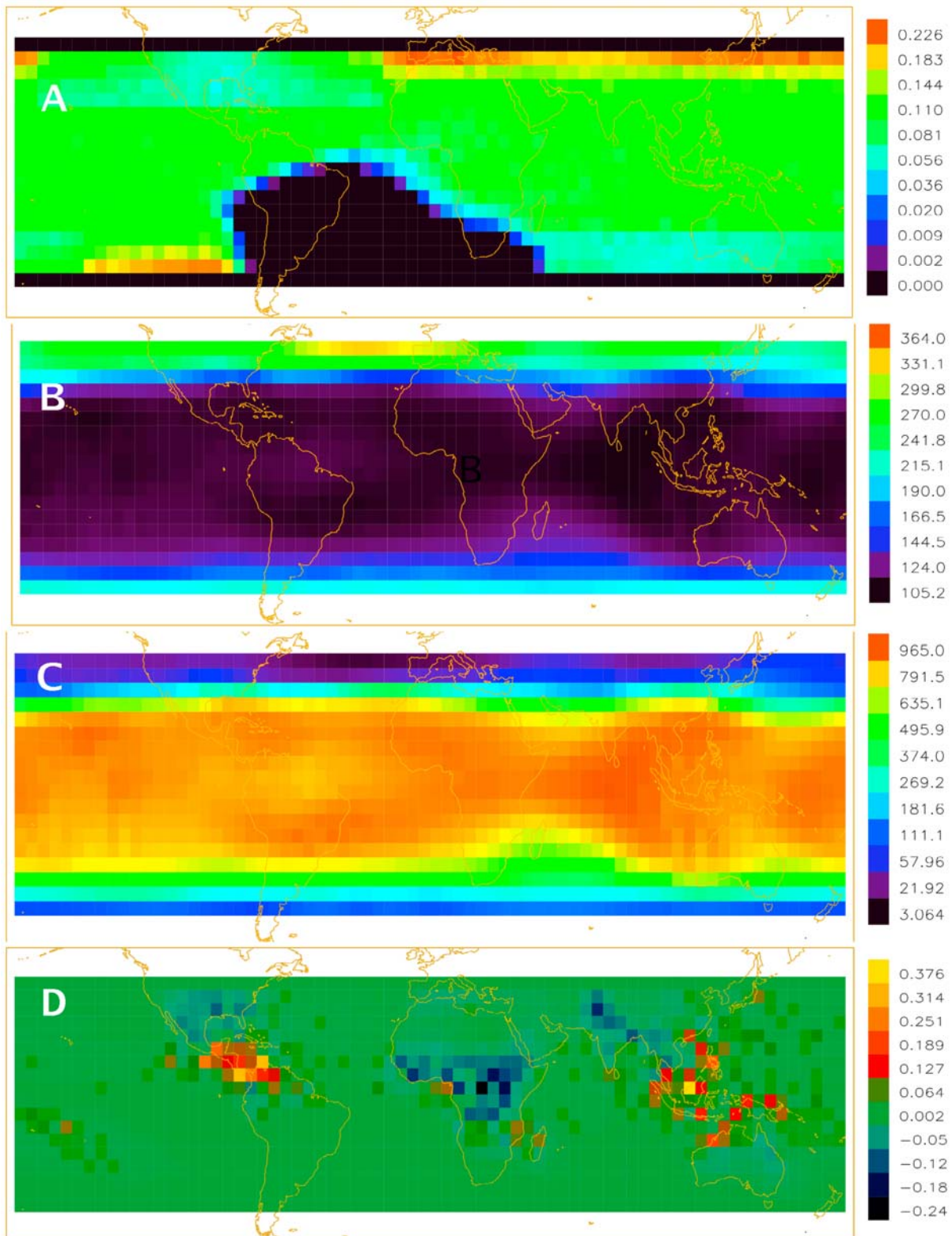


Figure 5. Auxiliary maps for the comparison of the LIS/OTD lightning map with the RHESSI TGF map. (a) RHESSI exposure/efficiency map. This is a relative measure, and the absolute values are arbitrary. (b) Sample monthly NCEP/NCAR tropopause height map (January). The scale is in g cm^{-2} of overlying air mass (see text). (c) Sample monthly gamma ray transmission map based on tropopause height (January). The values on the scale have an arbitrary normalization but represent relative transmission values for TGF photons, based on Monte Carlo simulations (see text). (d) Difference between the TGF map (Figure 4d) and transmission-corrected lightning map (Figure 4c).

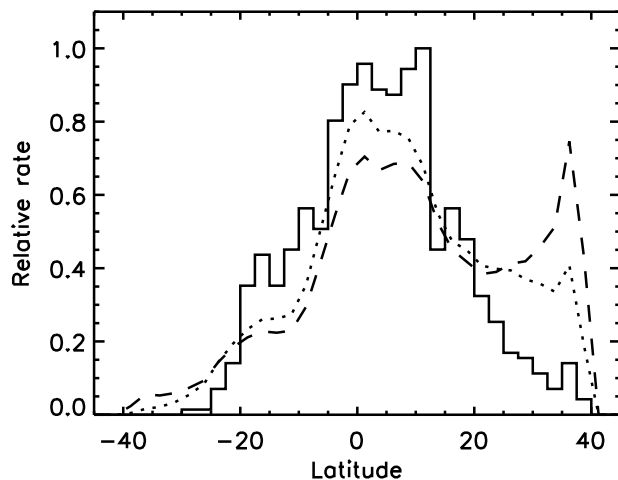


Figure 6. Latitude variation, summed over all longitudes, of the RHESSI TGF map (histogram), LIS/OTD lightning map corrected for RHESSI exposure (dashed line), and LIS/OTD map corrected for both RHESSI exposure and gamma ray attenuation from the tropopause (dotted line). These correspond to the maps in Figures 4d, 4b, and 4c, respectively.

detectors saturate during about half of TGFs [Grefenstette *et al.*, 2009], and if TGFs in Africa were actually brighter than most others, they could paralyze the detectors to the point where fewer counts registered than would be the case for a fainter event. This would be particularly likely in events on the short end of the TGF duration distribution; we require at least 17 detected gammas to identify a TGF, and for a very short, bright event the instrumental dead time could prevent this many from being collected. If this bias against short and bright events were operating more severely in Africa than elsewhere due to higher gamma fluxes there, we would expect to find African TGFs registered by RHESSI longer in duration on average than TGFs elsewhere, since a long event can provide enough total counts even when instrumental dead time is high. Figure 8 shows histograms of TGF duration for the 205 African TGFs and the 638 occurring elsewhere. The average (detected) African TGF is indeed slightly longer, $725 \mu\text{s}$ versus $636 \mu\text{s}$. To determine the significance of this difference, we iterated a process of selecting arbitrary subsamples of 205 and 638 TGFs from

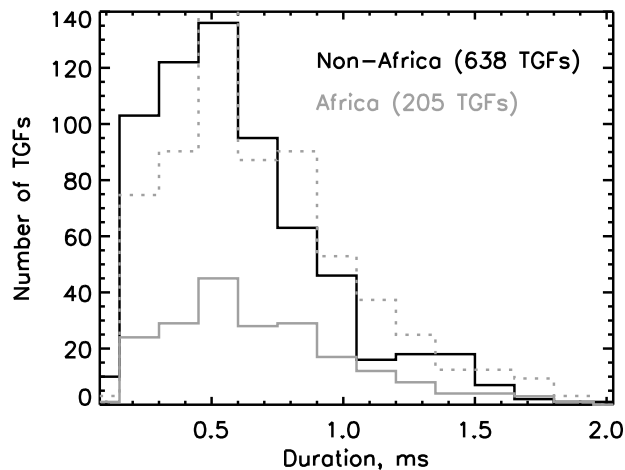


Figure 8. Histograms of TGF duration for African and non-African TGFs. The dotted line shows the African histogram scaled to the same number of events as the non-African distribution.

the overall population and finding the difference of their average durations. The difference was greater than $89 \mu\text{s}$ only 0.55% of the time. This supports the notion of the short African TGFs being suppressed by their brightness, although we cannot rule out the possibility that Africa really does have fewer TGFs, if they also happen to be genuinely longer than average.

[26] The TGF-poor regions in the United States and south to central Asia are high-latitude regions for lightning production, with generally low tropopause heights. One possible explanation for the remaining disagreement in these two regions is that TGFs could originate from well below the tropopause. If typical TGFs occurred at a certain distance below the tropopause, the transmission correction should be steeper than what we derived, since the gradient in atmospheric density increases at lower altitudes. This would result in greater suppression of the high latitudes, but would have other implications. The expected tropopause pressures associated with the majority of TGFs (Figure 9) correspond to altitudes of about 15.0–16.5 km. This is already toward the lower end of the range derived from spectroscopy of RHESSI TGFs by Dwyer and Smith [2005], so a much lower source would result in a conflict with that independent

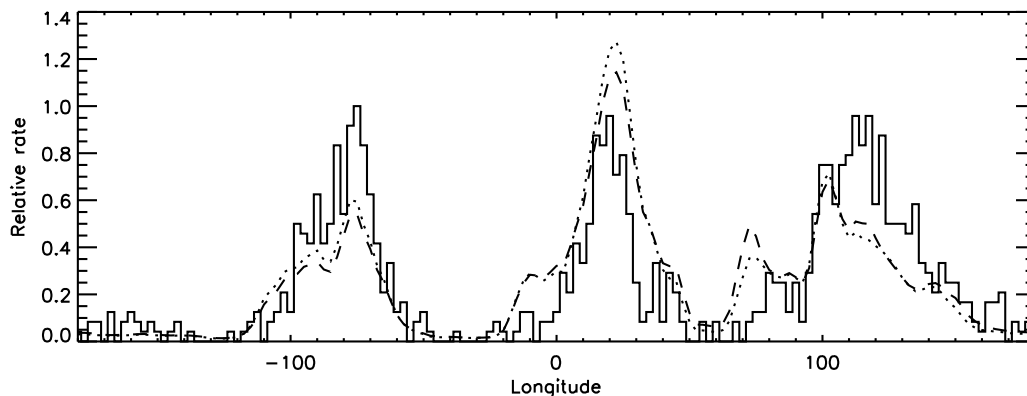


Figure 7. Longitude distributions summed over latitude for the same three cases shown in Figure 6.

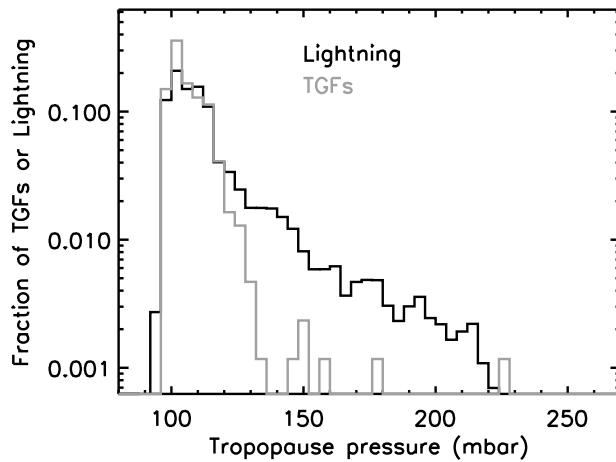


Figure 9. Histograms of tropopause pressure (mbar) for TGFs (gray) and lightning (black), showing the preference of TGFs for high altitudes.

method. Much deeper sources would also require extremely large total energies for the TGFs to still be seen from space. If TGFs occurred at a typical pressure (or mass) offset below the tropopause, instead of a typical distance, there would be no change in the relative transmission factors in Figure 5c.

[27] The final major difference between the modified lightning map and the TGF map, for which we offer no specific hypothesis at present, is a distinct eastward shift in the TGF peak relative to lightning in the Maritime Continent. We conclude that while the differential absorption effect due to differing tropopause heights plays a significant role in reconciling the TGF and lightning maps, at least half of the difference requires other explanations (see Figures 4c, 4d, 5d, 6 and 7).

4.2. Tropopause Height Distribution and Individual Events

[28] Figure 9 shows the distribution of expected tropopause heights for each TGF (using the NCEP data for the position and month of its occurrence). For comparison, we created histograms of tropopause-height distributions for the monthly NCEP maps, using each month's LIS/OTD map as a weighting factor, to give a corresponding tropopause-height distribution for total lightning. The difference is dramatic. Except for a small number of exceptional events, the TGFs

are almost exclusively at the higher tropopause altitudes. Note, however, that most lightning is also associated with a high tropopause; the scale is logarithmic. Thus the TGFs are not occurring only in times and places with the very highest expected tropopause; rather, it is just the low-tropopause tail of lightning that is missing. It is an open question whether TGFs are a rare occurrence or whether most are simply "hidden" at low altitudes. Figure 9 cannot resolve that question, since it addresses only mean expected tropopause heights and ignores two factors: the distribution of storm heights around the mean expected tropopause and the distribution of lightning with altitude in a given storm, from CG lightning up to IC lightning and perhaps even upward lightning (e.g., blue jets) that could transfer charge to altitudes well above the tropopause. In principle any of these regions could produce relativistic runaway and gammas.

[29] One exceptional TGF has an expected tropopause that is not only lower than the usual value when a TGF is observed, but lower than the values expected when nearly all lightning is seen (226 mbar in Figure 9). This event was on the Virginia coast of the United States at 04:08:06.740 UT on 30 March 2003; the early date for a North American thunderstorm explains the very low expected tropopause height. The National Weather Service Storm Data and Unusual Weather Phenomena document for this date (available at <http://www.ncdc.noaa.gov/oa/climate/sd/>) describes penny-sized hail and tornadoes in the area 4.5 h before the TGF. GOES 8 infrared imagery (courtesy of the Earth Science Office at NASA/Marshall Space Flight Center) shows larger areas of cold cloud tops at the time of the TGF than were present at the time of the tornadoes.

[30] Figure 10 shows the positions of the 6 TGFs with the lowest expected tropopause heights (>140 mbar). Three more of these, in addition to the 30 March 2003 event, are off the Atlantic coast of the United States, in June 2002, May 2003, and May 2004. We plan further meteorological studies of these storms to see if they had unusually high tropopause heights or large overshooting tops, and to determine if this region is particularly susceptible to such behavior early in the thunderstorm season.

5. Conclusion

[31] We have demonstrated that TGFs tend to occur during times when the flash rate seen by WWLLN is declining, when considering a 40 min period centered on the TGF. This

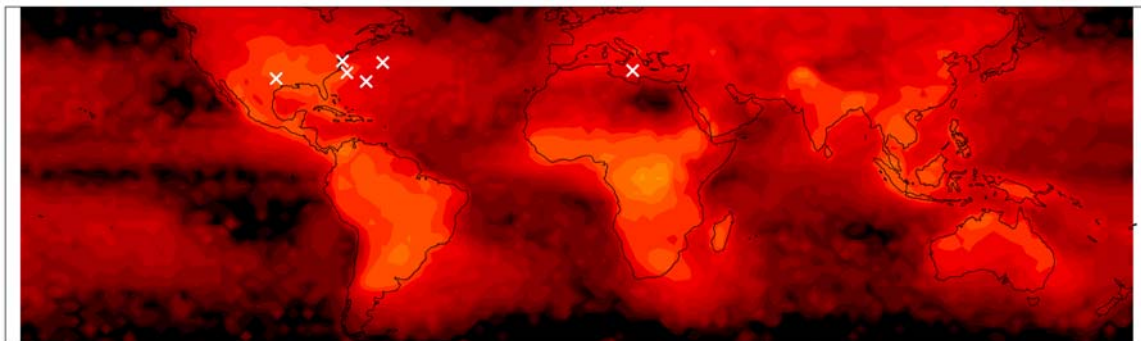


Figure 10. Position of the six TGFs with tropopause pressures >140 mbar; see Figure 5. The brightness scale beneath is another rendering of the LIS/OTD map (Figure 4a).

is contrary to the expectation for +IC lightning, and may suggest either a wider variety of parent lightning for TGFs, including +CG flashes, or else that TGFs are associated with some very particular subset of +IC lightning that does not follow the same evolution through a storm as the bulk of +IC flashes. The analysis was limited by the lack of position resolution of RHESSI, so that only a small subsample of the RHESSI TGFs, those corresponding to compact, isolated clusters of WWLLN sferics, could be used. The ability to localize the TGF, e.g., by detecting its sferic with an array more sensitive to very small charge-moment changes, would greatly improve the statistics of this analysis.

[32] We used NCEP/NCAR reanalysis data to find an expected tropopause height for the calendar month and location of each TGF. With a few exceptions, TGFs tended to occur in times and places when the tropopause is high. This is true of lightning as well, since both lightning and tropopause height peak during local summer, but the low-tropopause “tail” of lightning (essentially winter lightning) does not appear in the TGF distribution. Several of the exceptional TGFs at low tropopause heights cluster off the Eastern seaboard of the United States (Figure 10). No two are from the same storm system, so this seems to be a persistent trend in this region. The effect described by Williams *et al.* [2006], that low-altitude TGFs will be detected less often from space because the gamma rays are absorbed in the atmosphere, is partially supported by the TGF map. Including this effect brings the TGF map into closer agreement with the LIS/OTD lightning map, but there are still significant differences. In Figure 9, the distribution of tropopause heights corresponding to TGFs departs strongly from the corresponding distribution for lightning between 120 and 140 mbar. This corresponds to 26 g cm^{-2} , or a loss of about a factor of two in the photons escaping to space. If many of the RHESSI TGFs are saturating the instrument anyway [Grefenstette *et al.*, 2009], then a factor of two in absorption should not prevent the detection of a majority of TGFs at 140 mbar. This suggests other factors related to regional meteorology that cause the differences between TGFs and lightning in Figures 5d, 6, 7, and 9. Understanding these regional differences may lead to a better understanding of the physical conditions conducive to TGFs and therefore the TGF mechanism.

[33] **Acknowledgments.** We thank the referees for constructive and thought-provoking suggestions. This work makes use of the public v1.0 gridded LIS/OTD data. These data were produced by the NASA Lightning Image Sensor/Optical Transient Detector Science Team (Principal Investigator H. J. Christian, NASA/Marshall Space Flight Center) and are available from the Global Hydrology Resource Center (<http://ghrc.msfc.nasa.gov>). NCEP Reanalysis Derived data were provided by the NOAA/OAR/ESRL PSD, Boulder, Colorado, USA, from their Web site at <http://www.cdc.noaa.gov/>. The authors wish to thank the World Wide Lightning Location Network (<http://wwlln.net>), a collaboration among over 40 universities and institutions, for providing the lightning location data used in this paper. This work was supported in part by NSF grant ATM0607885 and NASA contract NAS5-98033.

[34] Amitava Bhattacharjee thanks James Brundell and Ken Eack for their assistance in evaluating this paper.

References

- Brunetti, M., S. Cecchini, M. Galli, G. Giovannini, and A. Pagliarini (2000), Gamma-ray bursts of atmospheric origin in the MEV energy range, *Geophys. Res. Lett.*, **27**, 1599–1602.
- Carlson, B. E., N. G. Lehtinen, and U. S. Inan (2009), Terrestrial gamma ray flash production by lightning current pulses, *J. Geophys. Res.*, **114**, A00E08, doi:10.1029/2009JA014531.
- Cummer, S. A., Y. Zhai, W. Hu, D. M. Smith, L. I. Lopez, and M. A. Stanley (2005), Measurements and implications of the relationship between lightning and terrestrial gamma ray flashes, *Geophys. Res. Lett.*, **32**, L08811, doi:10.1029/2005GL022778.
- Dwyer, J. R. (2003), A fundamental limit on electric fields in air, *Geophys. Res. Lett.*, **30**(20), 2055, doi:10.1029/2003GL017781.
- Dwyer, J. R. (2008), Source mechanisms of terrestrial gamma-ray flashes, *J. Geophys. Res.*, **113**, D10103, doi:10.1029/2007JD009248.
- Dwyer, J. R., and D. M. Smith (2005), A comparison between Monte Carlo simulations of runaway breakdown and terrestrial gamma-ray flash observations, *Geophys. Res. Lett.*, **32**, L22804, doi:10.1029/2005GL023848.
- Dwyer, J. R., B. W. Grefenstette, and D. M. Smith (2008), High-energy electron beams launched into space by thunderstorms, *Geophys. Res. Lett.*, **35**, L02815, doi:10.1029/2007GL032430.
- Eack, K. B., W. H. B., W. D. Rust, T. C. Marshall, and M. Stolzenburg (1996a), Initial results from simultaneous observation of X-rays and electric fields in a thunderstorm, *J. Geophys. Res.*, **101**, 29,637–29,640.
- Eack, K. B., W. H. Beasley, W. D. Rust, T. C. Marshall, and M. Stolzenburg (1996b), X-ray pulses observed above a mesoscale convective system, *Geophys. Res. Lett.*, **23**, 2915–2918.
- Eack, K. B., D. M. Suszeynsky, W. H. Beasley, R. A. Roussel-Dupré, and E. Symbalisty (2000), Gamma-ray emission observed in thunderstorm anvil, *Geophys. Res. Lett.*, **27**, 185–188.
- Fishman, G. J., et al. (1994), Discovery of intense gamma-ray flashes of atmospheric origin, *Science*, **264**, 1313–1316.
- GEANT Team (1993), GEANT—Detector description and simulation tool, CERN program library long write-up W5013, technical report, CERN, Geneva.
- Grefenstette, B. W., D. M. Smith, B. J. Hazelton, and L. I. Lopez (2009), First RHESSI terrestrial gamma ray flash catalog, *J. Geophys. Res.*, **114**, A02314, doi:10.1029/2008JA013721.
- Hazelton, B. J., B. W. Grefenstette, D. M. Smith, J. R. Dwyer, X.-M. Shao, S. A. Cummer, T. Chronis, E. H. Lay, and R. H. Holzworth (2009), Spectral dependence of terrestrial gamma-ray flashes on source distance, *Geophys. Res. Lett.*, **36**, L01108, doi:10.1029/2008GL035906.
- Humphreys, W. J. (1964), *Physics of the Air*, Dover, New York.
- Inan, U. S., S. C. Reising, G. J. Fishman, and J. M. Horack (1996), On the association of terrestrial gamma-ray bursts with lightning and implications for sprites, *Geophys. Res. Lett.*, **23**, 1017–1020.
- Inan, U. S., M. B. Cohen, R. K. Said, D. M. Smith, and L. I. Lopez (2006), Terrestrial gamma ray flashes and lightning discharges, *Geophys. Res. Lett.*, **33**, L18802, doi:10.1029/2006GL027085.
- Jacobson, A. R., R. H. Holzworth, J. Harlin, R. L. Dowden, and E. H. Lay (2006), Performance assessment of the World Wide Lightning Location Network (WWLLN) using the Los Alamos Sferic Array (LASA) as ground truth, *J. Atmos. Oceanic Technol.*, **23**, 1082–1092.
- Kalnay, E., et al. (1996), The NCEP/NCAR 40-year reanalysis project, *Bull. Am. Meteorol. Soc.*, **77**, 437–470.
- Lay, E. H., R. H. Holzworth, C. J. Rodger, J. N. Thomas, O. Pinto Jr., and R. L. Dowden (2004), WWLLN global lightning detection system: Regional validation study in Brazil, *Geophys. Res. Lett.*, **31**, L03102, doi:10.1029/2003GL018882.
- Lay, E. H., R. H. Holzworth, C. J. Rodger, A. R. Jacobson, L. I. Lopez, and D. M. Smith (2005), Using WWLLN to provide insight on terrestrial gamma-ray flashes, poster presented at 2005 Joint CEDAR-GEM Workshop, Coupling, Energetics and Dyn. of Atmos. Reg., Santa Fe, N. M.
- McCarthy, M., and G. K. Parks (1985), Further observations of X-rays inside thunderstorms, *Geophys. Res. Lett.*, **12**, 393–396.
- Moss, G. D., V. P. Pasko, N. Liu, and G. Veronis (2006), Monte Carlo model for analysis of thermal runaway electrons in streamer tips in transient luminous events and streamer zones of lightning leaders, *J. Geophys. Res.*, **111**, A02307, doi:10.1029/2005JA011350.
- Parks, G. K., B. H. Mauk, R. Spiger, and J. Chin (1981), X-ray enhancements detected during thunderstorm and lightning activities, *Geophys. Res. Lett.*, **8**, 1176–1179.
- Rodger, C. J., S. Werner, J. B. Brundell, E. H. Lay, N. R. Thomson, R. H. Holzworth, and R. L. Dowden (2006), Detection efficiency of the VLF World-Wide Lightning Location Network (WWLLN): Initial case study, *Ann. Geophys.*, **24**, 3197–3214.
- Rodger, C. J., J. B. Brundell, R. H. Holzworth, E. H. Lay, and R. L. Dowden (2008), Improvements in the WWLLN network: Growing detection efficiencies for “big lightning” events, paper presented at Workshop on Coupling of Thunderstorms and Lightning Discharges to Near-Earth Space, Univ. of Corsica, Corte, France.

- Shao, X.-M., T. D. Hamlin, and D. M. Smith (2010), A closer examination of terrestrial gamma-ray flash-related lightning processes, *J. Geophys. Res.*, doi:10.1029/2009JA014835, in press.
- Splitt, M. E., S. M. Lazarus, D. Barnes, J. R. Dwyer, H. K. Rassoul, D. M. Smith, B. J. Hazelton, and B. W. Grefenstette (2010), Thunderstorm characteristics associated with RHESSI-identified terrestrial gamma-ray flashes, *J. Geophys. Res.*, doi:10.1029/2009JA014622, in press.
- Stanley, M. A., X.-M. Shao, D. M. Smith, L. I. Lopez, M. B. Pongratz, J. D. Harlin, M. Stock, and A. Regan (2006), A link between terrestrial gamma-ray flashes and intracloud lightning discharges, *Geophys. Res. Lett.*, *33*, L06803, doi:10.1029/2005GL025537.
- Torii, T., M. Takeishi, and T. Hosono (2002), Observation of gamma-ray dose increase associated with winter thunderstorm and lightning activity, *J. Geophys. Res.*, *107*(D17), 4324, doi:10.1029/2001JD000938.
- Tsuchiya, H., et al. (2007), Detection of high-energy gamma rays from winter thunderclouds, *Phys. Rev. Lett.*, *99*, 165002, doi:10.1103/PhysRevLett.99.165002.
- Williams, E., et al. (2006), Lightning flashes conducive to the production and escape of gamma radiation to space, *J. Geophys. Res.*, *111*, D16209, doi:10.1029/2005JD006447.
- Williams, E. R., M. E. Weber, and R. E. Orville (1989), The relationship between lightning type and convective state of thunderclouds, *J. Geophys. Res.*, *94*, 13,213–13,220.
- Wilson, C. T. R. (1925), The electric field of a thundercloud and some of its effects, *Proc. Phys. Soc. London*, *32D*, 37.
-
- J. R. Dwyer, Department of Physics and Space Science, Florida Institute of Technology, 150 W. University Blvd., Melbourne, FL 32901, USA.
- B. W. Grefenstette, B. J. Hazelton, and D. M. Smith, Physics Department and Santa Cruz Institute for Particle Physics, University of California, Santa Cruz, 1156 High St., Santa Cruz, CA 95064, USA. (dsmith@scipp.ucsc.edu)
- R. H. Holzworth, Department of Earth and Space Sciences, University of Washington, 070 Johnson Hall, Box 351310, Seattle, WA 98195, USA.
- E. H. Lay, Los Alamos National Laboratory, MS D436, Los Alamos, NM 87545, USA.